Closed-Loop Current-Feedback, Signal-Chopped, Low Noise AMR Sensor With High Linearity

N. Hadjigeorgiou*, E. Hristoforou, P. P. Sotiriadis
School of Electrical and Computer Engineering
National Technical University of Athens (NTUA)
Athens, Greece
*nhatzig@central.ntua.gr

***Abstract*—Over the past twenty years' magnetic sensors have emerged as a preferred choice in many sensory systems due to their high accuracy, reliability and mechanical robustness. This has sparked the development of different types of magnetic sensors for magnetic field measurements as well as for measuring other quantities indirectly. Sensitivity, linearity, signal-to-noise ratio, measurement range and cross-talk between sensors in mutli-axis / multi-sensor applications are only some of the magnetic sensor's characteristics that have been studied in the past. The aim of this paper is to present a fully analog current-feedback closed loop system for AMR (Anisotropic Magnetic Resistance) magnetic sensors. The calibration and testing were conducted in a 3D Helmholtz coil setup capable of controlling the magnetic field amplitude and direction in the AMR sensor area. The noise characterization was realized in a multilayer tube of soft magnetic material. Thorough experimental characterization and testing indicates that the proposed close loop architecture improves sensor's linearity while maintaining low noise level.**

Keywords*— AMR sensor; closed loop; chopper; linearity improvement; sensitivity improvement; magnetic noise; electronic noise

I. INTRODUCTION

Magnetic sensors can be classified with respect to several of their characteristics. Their sensing principle though is the main aspect as it determines their operating characteristics such as resolution, measurement range, working temperature, frequency range and production cost. For instance, Flux-Gate sensors have been proven useful in water and space applications where accuracy is important and large environmental temperature variations are present. However, Flux-Gate sensors are not appropriate for low cost application or for high frequency magnetic field measurements [1].

On the other hand, Hall-effect sensors and search-coils have been proven to be cost effective in numerous applications. However, Hall-effect sensors drift significantly requiring compensation, whereas search coils cannot be used for low frequency magnetic field measurements.

A promising alternative option is the Anisotropic Magneto - Resistance (AMR) sensors as they offer a good compromise between cost and performance. AMR sensors can work from DC up to MHz frequency range, much higher than their competitive Flux-Gate sensors which also suffer from strong hysteresis effects. Moreover, AMR sensors have better resolution and lower noise than Hall effect sensors [2-4].

The Wheatstone bridge structure is the preferable topology for AMR sensors which are manufactured using magneto-resistive thin-film permalloy (NiFe) materials. The AMR sensors have high spatial resolution compared to Flux-Gate and other sensors since they are only a few μm in size. This is why they had been used in hard-drive heads for decades.

Many techniques have been introduced in the literature to boost the performance of AMR sensors. Techniques dealing with the suppression of the DC offset using digital feedback or implementation of a current pulsing circuit to accomplish the re-polarization of permalloy thin-film magnetic domains are the most common ones that can been found [3-5].

In addition, the cross-axis effect can be reduced by signal processing numerical as well as experimental techniques [6-8]. However, two important issues: the non-linear response and measurement noise of AMR sensors are often discussed very briefly leaving a lot to be desired.

Typically, either open-loop architectures or digital closed loop ones are used in AMR sensors. The first one suffers from non-linearity and increased noise whereas the second one, which improves on the linearity and noise, suffers from small operating bandwidth, orders of magnitudes smaller than that of the AMR sensor element.

In this paper, an analog, *current* - feedback closed loop architecture is proposed, developed and tested to minimize the non-linearity of AMR response and suppress the 1/f noise, improving the accuracy of magnetic field measurements. The measurements demonstrate that AMR response had a maximum deviation of 0.4‰ with respect to the ideal linear response. Moreover, the proposed current-feedback close-loop system demonstrated a noise figure almost as low as the corresponding intrinsic noise density of the AMR sensing element provided by the manufacturer [9].

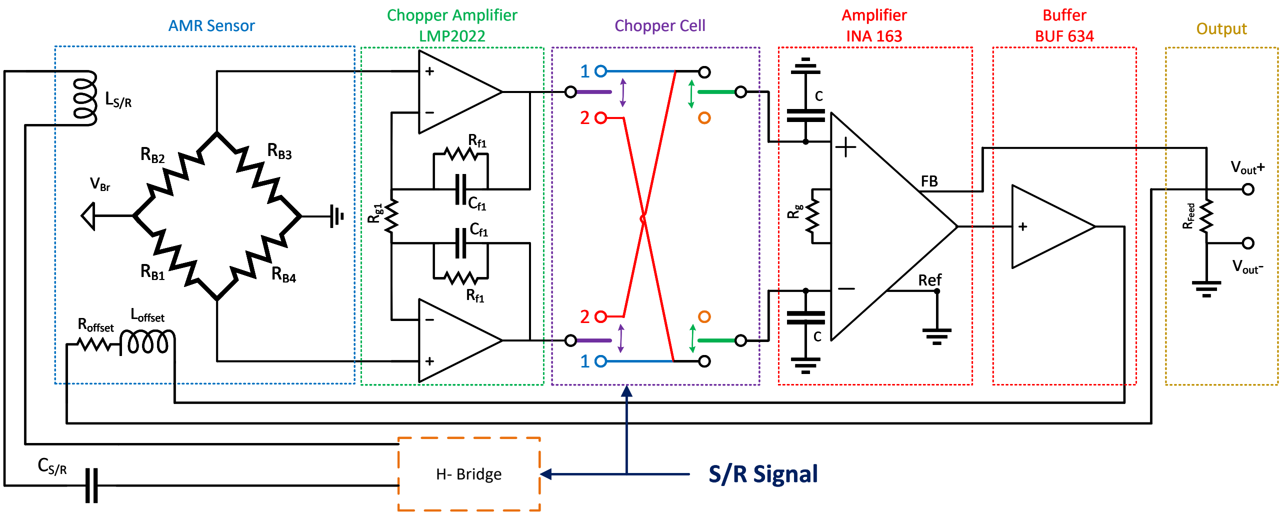

Fig 1: The proposed current-feedback closed loop architecture.

II. Proposed Current-Feedback Closed-Loop Architecture

For the purposes of this work, the HMC-1001 and 1002 AMR sensor elements, manufactured by Honeywell Inc., have been used. The structure of the proposed current closed loop system is illustrated in Fig.1

The system is composed of the AMR Wheatstone bridge sensor elements and the accompanying electronic circuitry, all of which are discussed briefly in the following subsections.

Notice the presence of two (integrated) coils in the AMR sensor element. The bottom one, L_{offset} is used for feedback purposes to improve linearity and reduce memory effects. The top-left one, $L_{S/R}$, is the set-reset coil used for the re-polarization of permalloy thin-film magnetic domains with short but strong current pulses. The source of those pulses is the H-Bridge using a capacitor in series. When a *set pulse* is given the voltage output of the sensor is F(B); it switches to -F(B) when a *reset pulse* is given. The chopper cell between the two amplifying stages reverses the polarity according to the set-reset pulses.

The complex of the instrumentation amplifier (INA 163), the voltage buffer (BUF 634) and the resistor (R_{feed}) forms the transconductor providing the current to the feedback offset strap.

A. The AMR Sensor Model

A simplified linear analytical model of the HMC-1001/2 sensor elements has been developed in order to obtain a first order approximation of sensors system frequency response and closed loop stability. This model is presented in Fig 2.

The model includes two signal paths: 1) The forward one, $H_{sen}(s)$, representing the transfer function of the conversion of the magnetic field intensity to voltage; it captures the inherent bandwidth of the sensing element using a simplified dominant-pole model, i.e. $H_{sen}(s)=\frac{2\pi f_{sen-3dB}}{s+2\pi f_{sen-3dB}}$.

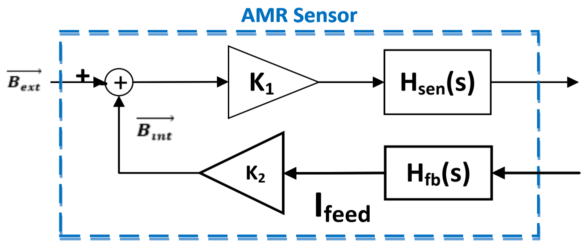

Fig. 2: Simplified analytic HMC-1001/2 sensor diagram.

2) The feedback path $H_{fb}(s)$ capturing the voltage to magnetic field intensity conversion via the offset coil $H_{fb}(s)=1/\left(sL_{offset}+R_{offset}\right)$. Constants K_1 and K_2 stand for the conversion gain ratios according to the datasheet [9].

B. System Model of the Closed Loop Architecture

The model of the analog circuitry, implementing the signal conditioning and closed loop operation, was developed. The circuit is divided into two main stages: 1) The chopper voltage amplification (LMP2022 chopper opamp); in this stage the sensor's output voltage is amplified, while maintaining the 1/f noise level as low as possible. 2) and a Transconductance (a voltage to current amplification) (INA 136, BUF634, R_{feed}); this stage provides the high output current needed to drive the internal compensation coil of the sensor element and implement the closed loop architecture. Fig 2.

Fig. 3 shows the complete system model of the electronic circuit along with the sensor's model. The transfer function of the amplifying stages $H_i(s)$, $i=1,2,3$ are given by

$$H_1(s)\approx\frac{A\cdot\left(s\cdot R_f\cdot C_f\cdot R_g+2\cdot R_f+R_g\right)}{\left((A+1)\cdot R_g\cdot R_f\cdot C_f\right)\cdot s+(A+1)\cdot R_g+2R_f} \tag{1}$$

$$H_2(s)\approx\frac{A\cdot\left(s\cdot R_f\cdot R_g+2\cdot R_f+R_g\right)}{\left((A+1)\cdot R_g\cdot R_f\right)\cdot s+(A+1)\cdot R_g+2R_f} \tag{2}$$

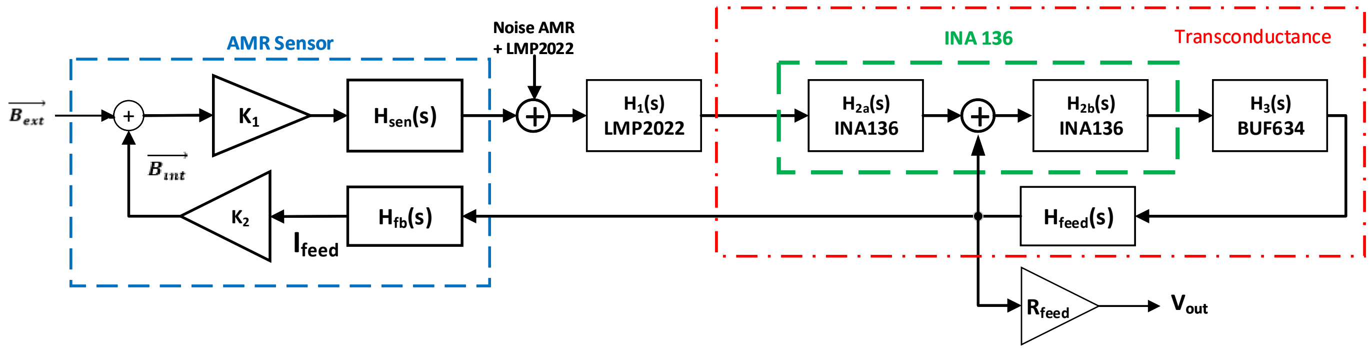

Fig. 3: Simplified analytic system diagram.

$$H_3(s) \approx \frac{0.95\cdot\left(2\cdot\pi\cdot180\cdot10^6\right)}{s+\left(2\cdot\pi\cdot180\cdot10^6\right)} \tag{3}$$

and the remaining feedback loop behavior is captured by

$$H_{feed}(s) = \frac{1}{R_{Feed}} \tag{4}$$

$$H_{Transcond}(s) \approx \frac{1}{R_{Feed}}\cdot\frac{5\cdot\left(2\cdot\pi\cdot250\cdot10^3\right)}{s+\left(2\cdot\pi\cdot250\cdot10^3\right)} \tag{5}$$

The output voltage noise power spectral density of $H_1(s)$ is $E_{H1} \approx 7{,}7\,\mu V/\sqrt{Hz}$. Finally, Eq. 6 gives the complete transfer function

$$\begin{aligned} H_{Total} &\approx \frac{K_1\cdot H_{sen}\cdot H_1\cdot H_{Transc}\cdot R_{feed}}{1+K_1\cdot K_2\cdot H_{sen}\cdot H_{fb}\cdot H_1\cdot H_{Transc}} \\ H_{Total} &\approx \frac{13750\cdot2\cdot\pi\cdot14.5\cdot10^3}{s+2\cdot\pi\cdot14.5\cdot10^3}\left(\frac{Volt}{Tesla}\right) \end{aligned} \tag{6}$$

and the closed loop noise density at 1Hz is

$$E = 61\,\mu V/\sqrt{Hz}\ \ @\ 1\text{Hz} \tag{7}$$

Referring the noise PSD in Eq. 7 to the input of the sensor system and using the result of Eq. 6, the closed loop noise density at the input is $4.45\,nT/\sqrt{Hz}$ @ 1 Hz. The integrated noise power from 0.1Hz up to 1KHz is 532nT RMS.

C. *Measurment Setup*

The experimental setup is consisted of two pieces of equipment, the *3D Helmholtz coil* and the *Degaussing chamber* with magnetic shield. The DC magnetic field measurements have been conducted in laboratory environment employing a Helmholtz coil setup in order to calibrate/characterize the system under consideration. The effective bandwidth of the system was identified by AC field measurements using the same setup. The magnetic shield which is made from a multilayer soft magnetic material was used for magnetic noise measurements.

III. Measuremments And Discussion

Every sensor system must be calibrated and characterized. This process is presented in the next section and is consisted of three steps. First step the "DC Measurements and Calibration" presents the result for the identification of the sensor as well as relationship between the magnetic field and the voltage output. It presents the deviation from linearity both for the system and the sensor. The second step is to determine the bandwidth of the sensor in the section "Frequency Response". Finally, the magnetic noise characterization over frequency is shown in the corresponding section. The latter is very important since it defines the resolution capability of the sensor.

A. *DC Measurments and Calibration.*

Using a high precision current source and the Helmholtz coils a controlled linear magnetic field was generated. Both the proposed closed loop sensor system and the sensor alone were tested in the same chamber.

Utilizing the least square method a first order correlation between the magnetic field and the voltage output was obtained. The gain coefficients (i.e. magnetic field in measured mVolt/μTesla) are given below for the closed loop (CL) and sensor (S) system respectively.

$$V_{CL_X} = 13.79\left(\tfrac{mV}{\mu T}\right)\cdot B + 2.1\left(mV\right) \qquad V_{S_X} = 0.155\left(\tfrac{mV}{\mu T}\right)\cdot B + 7.4\left(mV\right)$$

In order to observe the (DC) nonlinearity of the system and the sensor element, the linear components were subtracted from their curves and the remaining nonlinear components were normalized. The results are shown in Fig 4.

The advantage of the proposed current-feedback close loop sensor system can be seen in Fig 4. The experimental results indicate that this closed loop AMR sensor has a maximum deviation of 0.4‰ with respect to the ideal linear response.

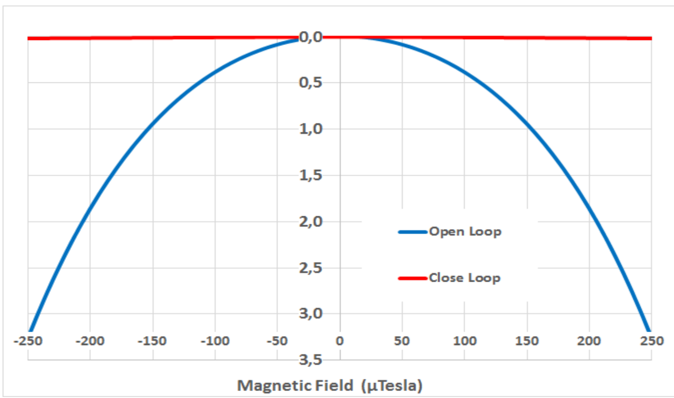

Fig. 4: Deviation from linearity (percentage) for the close loop system and for the sensor element.

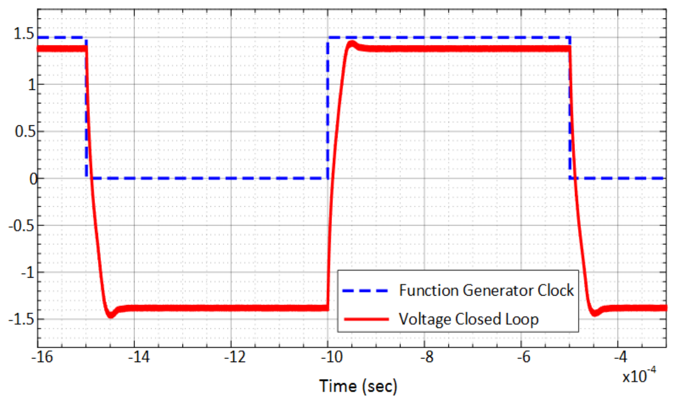

Fig. 5: Closed loop sensor step response at ±100µTesla.

B. *Frequency Response.*

The frequency response was derived by stimulating the Helmholtz coils with AC current. The provided current was generated by a (voltage-output) function generator driving a high precision voltage controlled current source (VCCS). Fig. 6 displays the frequency response of one axis (the response of the other two is similar). The experimental and the theoretical data are in good agreement.

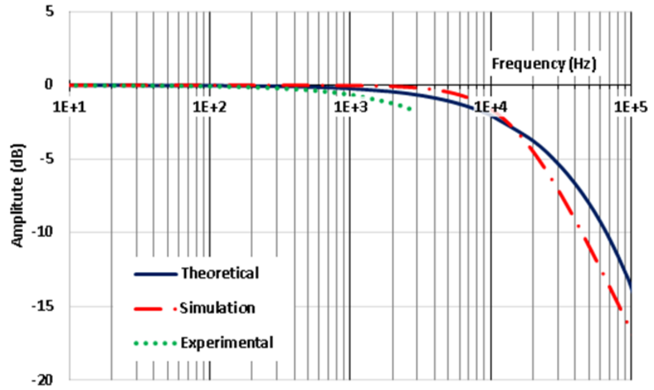

Fig. 6: AC Bandwidth Measurements.

The experimental data of AC analysis stop at 2.5KHz due to the Helmholtz coils inductance and the maximum voltage that the VCCS can give at 200 µTesla amplitude of magnetic field.

C. *Magnetic Noise Characterization*

In order to obtain the noise power spectral density, the closed loop system was placed inside the magnetic shield. The experimental results with respect to the noise of the sensor and the closed loop system, stimulated by a 100Hz magnetic field, are presented in the Fig. 7. Note that the waveform is shown in logarithmic scale and for small y-values the resolution of the recording instrument sets the quantization resolution of the measurement. The theoretical data were extracted through the datasheet of the sensor have also been included for comparison.

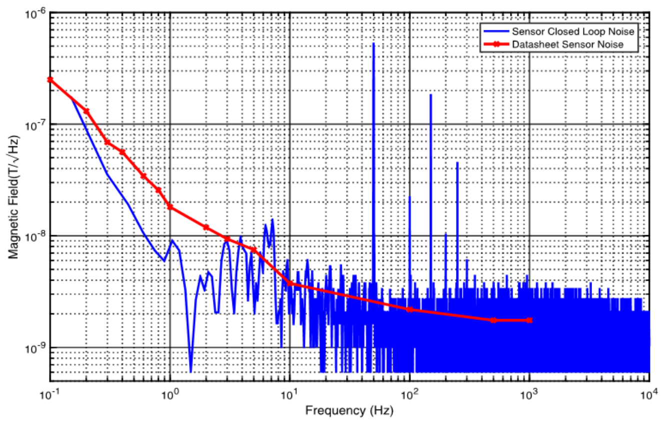

Fig. 7: Magnetic Noise Measurements.

IV. CONCLUSIONS

The experimental and the theoretical results of the closed loop AMR sensor system indicate that the proposed architecture can provide an alternative and cost effective solution for high precision measurements compared to more expensive sensors types like Flux-Gate. The system demonstrated good linearity while maintaining the magnetic noise levels of the sensor. Moreover, the effective bandwidth of the close loop system is wider compared to the other closed loop architectures of other AMR sensor systems found in the literature.

REFERENCES

[1] P. Ripka, Magnetic Sensors and Magnetometers. Artech House Publishers, 2001.

[2] F. Paixao, C. Quini, O. Baffa, J. Miranda, “A novel device with 36 channels for imaging and signal acquisition of the gastrointestinal tract based on AC biosusceptometry”, 2010 Annual International Conference of the IEEE Engineering in Medicine and Biology, Buenos Aires, 2010, pp. 6457-6460.

[3] S.S. Ibanez et al, “A Front-End ASIC for a 3-D Magnetometer for Space Applications by Using Anisotropic Magnetoresistors”, IEEE Transactions on Magnetics, vol. 51, pp. 1-4, January 2015.

[4] S. Leittner et al., “Design of the Magnetoresistive Magnetometer for ESA’s SOSMAG Project”, IEEE Transactions on Magnetics, vol. 51, pp. 1-4, January 2015.

[5] M. Janosek, J. Vyhnanek and P. Ripka, “CW Metal Detector Based on AMR Sensor Array”, Sensors, 2011 IEEE, Limerick, 2011, pp. 1515-1517.

[6] J. Chen, L. Yu, C. Zuo, X. Chen, S. Wu, X. Yang, “Compensation Method of Cross-axis Effect for AMR Sensor”, Electrical and Control Engineering (ICECE), 2010 International Conference on, Wuhan, 2010, pp. 603-606.

[7] K. Mohamadabadi, C. Coillot, M. Hillion, “New Compensation Method for Cross-Axis Effect for Three-Axis AMR Sensors”, IEEE Sensors Journal, vol. 13, no. 4, pp. 1355-1362, April 2013.

[8] L. Yu et al, "Error Compensation and Implementation of Embedded High-Precision Magnetometer", Electrical and Control Engineering (ICECE), 2010 International Conference on, Wuhan, 2010, pp. 911-914.

[9] Datasheet 1- and 2-Axis Magnetic Sensors HMC 1001/1002/1021/1022, www.aerospace.honeywell.com